A Fault Tolerant Control Model for AUV Thrusters under the Disabled Velocity Information Condition

Xiu-lian Liu, Li-dong Guo, Li-xin Yang, Jian-wei Zhu, Qi-qi Shen

Abstract—**Under the time-varying ocean current environment, the path tracking control is extremely complex when the AUV thruster faults or thruster saturation constraints occur. Different from the existing models with the inverse control method, a fault tolerant control method was proposed to AUV thrusters while its velocity information was not available. Considering the difficulty in constructing a high-fidelity dynamic model for the AUV and the changes in dynamic characteristics caused by thruster failures, a adaptive regression neural networks was used to estimate those unknown parts of the dynamic model. Meanwhile, to solve the unknown AUV velocity information caused by the measurement noise and the sensor faults, a sliding-mode observer was designed for those velocity variables, and the adaptive rate and control law was obtained through the Lyapunov stability theory. Finally, the AUV path tracking simulation was conducted on the thruster failures.**

Index Terms—**AUV (autonomous underwater vehicle); Fault tolerant control; Sliding mode observer; Ocean current; Thruster saturation constraints**

I. Introduction

Autonomous underwater robots（AUV）are currently the only equipment capable of entering deep sea areas for marine environment, resource exploration, and underwater operations [1-3]. Under the time-varying ocean current environment, AUV displays the highly nonlinear and the strong coupling characteristic between multi-freedom system. Because of this, the path tracking control of AUV has always been a hot research field of marine engineering [4, 5].

For improving the AUV's tracking accuracy, a variety of intelligent control methods have been shown in current research, including the neural network control [6, 7], the sliding mode control [8, 9], the fuzzy control [10], the inversion control [11], the adaptive control [12] and so on. Extensive simulation results show that those proposed methods can compensate the external disturbances caused by the ocean current and achieve better tracking accuracy. However, it is worth noting that most of those control methods are based on the overall measurable states of AUV, which means that the position and speed requirements can be directly obtained. In the practical applications, it has been found that the velocity information obtained by velocity sensors generally contains significant noise, especially for the doppler velocity log (DVL) sensors. Restricted by the doppler measurement principles, DVL is prone to significant measurement errors through external environmental influences. At this moment, when the velocity sensor malfunctions and applies to the control algorithm, the incorrect velocity information will lead to a deterioration of control performance. For example, the neural network sliding mode method can achieve depth control and good tracking performance through the measured position and velocity information. But its control output mutation phenomenon is extremely serious if there is large measurement noise and faults in the velocity sensor, which influences the performance of the thruster. Therefore, it is of meaningful to research the AUV path tracking control problem when the velocity information is unavailable.

To avoid the need for AUV speed information while maintaining high tracking accuracy, many literatures [13-16] have proposed state observer based the control methods. Su et al. [16] discussed the set-point control problem based on the AUV output feedback and proposed an inversion control method based on observer. Wang et al. [17] showed an AUV output feedback control method based on the equivalent output injection method. Reference [18] studied a fault-tolerant control method of AUV thrusters and adopted a state observer to obtain the velocity information for the unmeasurable conditions. In summary, it has been found that most observers require accurate AUV dynamic models. However, due to the nonlinearity, the strong coupling characteristics, and the disturbance of time-varying ocean currents, it is difficult to construct high fidelity and high confidence dynamic models [19, 20]. In addition, as the main driving component of AUV, the thruster works in seawater for a long time, which is prone to appear time-varying faults such as aging and insufficient output. In the course of the actual operation of AUV, the possible thruster failure will also cause changes in the dynamic model, thereby further affecting the tracking control effect.

Through the adaptive neural network model inversion, this paper proposes a fault-tolerant control method for AUV

Manuscript received November 13, 2023; revised November 7, 2024.

This work was supported in part by Scientific Research of Zhejiang Province Education Department of China under Grant Y202249228 and Y202145975, and High Level Talents Projects of Huzhou Vocational and Technical College under Grant 2022GY20 and 2022GY02.

Xiu-lian Liu is a Lecturer of Huzhou Vocational & Technical College, Zhejiang, Huzhou, China. (corresponding author to provide phone: 0086-572-2363622; fax: 0086-572-2363622; E-mail: liuchangrongghappy@yeah.net).

Li-dong Guo is a Lecturer of Huzhou Vocational & Technical College, Zhejiang, Huzhou, China. (E-mail: guozh075000@yeah.net).

Li-xin Yang is a Lecturer of Huzhou Vocational & Technical College, Zhejiang, Huzhou, China. (E-mail: yangli110159@yeah.net).

Jian-wei Zhu is an Associate Professor of Huzhou Vocational & Technical College, Zhejiang, Huzhou, China. (E-mail: zhujianwei18@yeah.net).

Qi-qi Shen is an Assistant of Huzhou Vocational & Technical College, Zhejiang, Huzhou, China. (E-mail: shenqq2056@yeah.net).

thrusters on account of adaptive neural network model inversion, of which can solve the AUV path tracking control problems in unknown and complex ocean current environments where the velocity information is unavailable, thruster faults occur, and thruster saturation constraints exist. Considering the difficulty in obtaining the accurate dynamic model and the accurate representation of the changes dynamic characteristics caused by the AUV thruster faults, an adaptive regression neural network is adopted to estimate those unknown dynamic components, thus achieving thruster fault-tolerant control without the need for AUV dynamic models and thruster fault diagnosis. This paper proposes a sliding mode observer to estimate the unavailable speed information in response to the significant measurement error of AUV speed state variables and the control problem caused by the unavailability of speed variables when the speed sensor fails. And that the adaptive rate and control law of neural networks are deduced through the Lyapunov stability theory. Finally, the application effect is validated through those path tracking simulations on the "ODIN" AUV.

II. MATHEMATICAL MODEL DESCRIPTION

A. AUV Dynamic Model

In the ship coordinate system, an AUV dynamic model considering thruster saturation constraints [21, 22] can be given by

$$\begin{aligned} &\dot{\boldsymbol{\eta}} = \boldsymbol{J}(\boldsymbol{\eta})\boldsymbol{v} \\ &\boldsymbol{M}\dot{\boldsymbol{v}} + \boldsymbol{C}_{RB}(\boldsymbol{v})\boldsymbol{v} + \boldsymbol{g}(\boldsymbol{\eta}) + \boldsymbol{C}_A(\boldsymbol{v}_r)\boldsymbol{v}_r + \\ &\quad \boldsymbol{D}_A(\boldsymbol{v}_r)\boldsymbol{v}_r = \boldsymbol{B}sat(u) - \boldsymbol{BK}sat(u) \end{aligned} \tag{1}$$

$$sat(u) = \begin{cases} u_{\max} & u > u_{\max} \\ u & u_{\min} < u < u_{\max} \\ u_{\min} & u < u_{\min} \end{cases} \tag{2}$$

The physical meanings of each variable in Eq. (1) and Eq. (2) are detailed in the literature [21,22].

Through converting Eq. (1) to the reference system, the state model is expressed as:

$$\ddot{\boldsymbol{\eta}} = \boldsymbol{G}(\boldsymbol{\eta}) \cdot sat(u) + \boldsymbol{F}(\boldsymbol{\eta}, \dot{\boldsymbol{\eta}}) \tag{3}$$

$$\begin{aligned} &\boldsymbol{G}(\boldsymbol{\eta}) = \boldsymbol{M}_\eta(\boldsymbol{\eta})^{-1}\boldsymbol{J}^{-\mathrm{T}}\boldsymbol{B} \\ &\boldsymbol{F}(\boldsymbol{\eta},\dot{\boldsymbol{\eta}}) = -\boldsymbol{M}_\eta(\boldsymbol{\eta})^{-1}\Big[\boldsymbol{C}_{RB\eta}(\boldsymbol{\eta},\dot{\boldsymbol{\eta}})\dot{\boldsymbol{\eta}} + \boldsymbol{C}_{A\eta}(\boldsymbol{\eta}_r,\dot{\boldsymbol{\eta}}_r)\dot{\boldsymbol{\eta}}_r + \\ &\quad \boldsymbol{D}_\eta(\boldsymbol{\eta}_r,\dot{\boldsymbol{\eta}}_r)\dot{\boldsymbol{\eta}}_r + \boldsymbol{g}_\eta(\boldsymbol{\eta}) - \boldsymbol{J}^{-T}\boldsymbol{BK}sat(u)\Big] \end{aligned} \tag{4}$$

$$\begin{aligned} &\boldsymbol{M}_\eta(\boldsymbol{\eta}) = \boldsymbol{J}^{-\mathrm{T}}\boldsymbol{M}\boldsymbol{J}^{-1}, \ \ \boldsymbol{\eta}_r = \boldsymbol{\eta} - \boldsymbol{V}_c \\ &\boldsymbol{C}_{RB\eta}(\boldsymbol{\eta},\dot{\boldsymbol{\eta}}) = \boldsymbol{J}^{-\mathrm{T}}[\boldsymbol{C}_{RB}(\boldsymbol{v}) - \boldsymbol{M}\boldsymbol{J}^{-1}\dot{J}]\boldsymbol{J}^{-1} \\ &\boldsymbol{C}_{A\eta}(\boldsymbol{\eta}_r,\dot{\boldsymbol{\eta}}_r) = \boldsymbol{J}^{-\mathrm{T}}\boldsymbol{C}_A(\boldsymbol{v}_r)\boldsymbol{J}^{-1} \\ &\boldsymbol{D}_\eta(\boldsymbol{\eta}_r,\dot{\boldsymbol{\eta}}_r) = \boldsymbol{J}^{-\mathrm{T}}\boldsymbol{D}(\boldsymbol{v}_r)\boldsymbol{J}^{-1} \\ &\boldsymbol{g}_\eta(\boldsymbol{\eta}) = \boldsymbol{J}^{-\mathrm{T}}\boldsymbol{g} \end{aligned} \tag{5}$$

Where $\boldsymbol{V}_c$ is vector of the ocean current in the Reference Coordinate System.

In this section, the basic assumption that the inertia matrix $\boldsymbol{M}_\eta(\boldsymbol{\eta})$ is known while the force matrix $\boldsymbol{F}(\boldsymbol{\eta},\dot{\boldsymbol{\eta}})$ is unknown.

B. Problem Description

Brief description of the expected objectives of the control model: For those AUV dynamic models given in Eq. (1) and Eq. (3), a fault-tolerant control model for AUV thrusters is established when considering ocean current interference, thruster failures and unavailable velocity information conditions. The implementation of the established method does not rely on the dynamic characteristic and can compensate for the ocean currents disturbance and the thruster faults on the overall system.

III. OBSERVER-BASED PATH TRACKING CONTROL METHOD

A. Control System Framework

Since accurate AUV dynamic models are difficult to obtain from the strong coupling characteristics among the working condition, the load and the AUV system sate, the traditional model inversion control methods can not realize the fault-tolerant control of AUV. Benefiting from nonlinear approximation ability of neural networks [19, 23-25], an adaptive regression neural networks is applied to estimate the unknown elements in the model inverse process. Through the Lyapunov stability theory, the adaptive rate of neural networks is also derived.

When using neural network model inversion method for AUV path tracking control, the velocity information is usually required. However, due to the measurement noise and other interference signals, as well as the time delay between the velocity information and the position information, an observer is designed for fault-tolerant control model of the AUV thrusters of which can estimate the unmeasurable velocity elements through a sliding mode observer.

B. Adaptive Neural Network Estimation

By using the nonlinear identification ability of neural networks, the unknown force matrix is constructed based on an adaptive regression neural network. Compared with feed-forward neural networks, and it can describe the time series information from input to output variables, the physical meanings of each variable in Equation (6) are detailed in the literature [19,23-26], as shown in Figure 1.

The network output can be described as:

$$f_o(N) = WQ(\boldsymbol{x},\alpha,\beta,\gamma) \tag{6}$$

Where: Q is hidden-layer output, and the activation function of hidden-layer neurons is described as $S(x) = 1/(1+\frac{1}{e^x})$; $\boldsymbol{x}$ is the input vector of the input layer node; α , β , γ and W are the weighting coefficients.

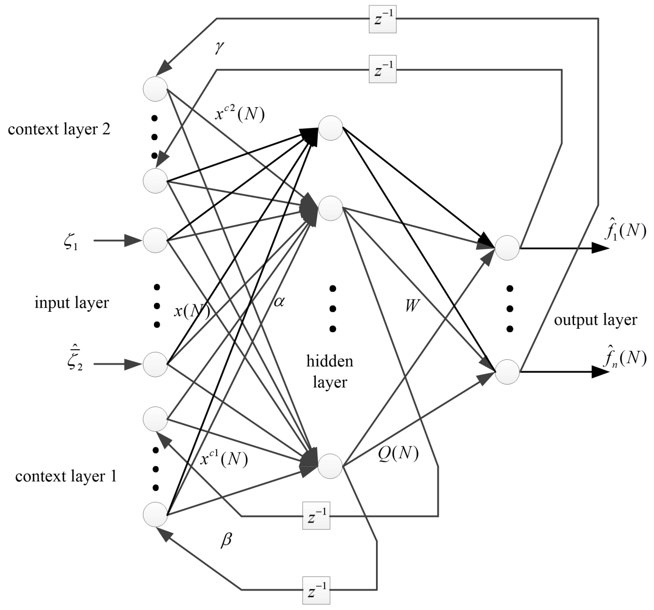

Fig. 1. Adaptive regression neural networks

Through the neural network, the unknown $\boldsymbol{F}(\boldsymbol{\eta},\dot{\boldsymbol{\eta}})$ can be determined by the optimal network weight value $W^*,\alpha^*,\beta^*,\gamma^*$ and given by:

$$\boldsymbol{F} = W^* Q(\zeta,\alpha^*,\beta^*,\gamma^*) + \varepsilon_f \tag{7}$$

Where: ε_f is the reconstruction error caused by the quantity of neures in the hidden and semantic layers of the neural network.

Using neural networks to estimate F, the estimated value can be expressed as

$$\hat{\boldsymbol{F}}_1 = \hat{W} Q(x,\hat{\alpha},\hat{\beta},\hat{\gamma}) \tag{8}$$

Where $\hat{W}$, and $\hat{\alpha},\hat{\beta},\hat{\gamma}$ are the estimated values of each weight value.

According to Eq. (7) and Eq. (8), the estimation error of the unknown elements $\boldsymbol{F}(\boldsymbol{\eta},\dot{\boldsymbol{\eta}})$ can be described as:

$$\begin{aligned}&\forall \tilde{Q} = Q^* - \hat{Q},\quad \tilde{W} = W^* - \hat{W}\\ &\tilde{\boldsymbol{F}} = \boldsymbol{F} - \hat{\boldsymbol{F}}_1 = W^*\tilde{Q} + \tilde{W}\hat{Q} + \varepsilon_f\end{aligned} \tag{9}$$

By conducting the Taylor expansion on the variable $\tilde{Q}$, then:

$$\begin{aligned}\tilde{Q} = &\left[\frac{\partial Q}{\partial(\alpha\zeta)}\right]^{\mathrm{T}} \tilde{\alpha}\zeta + \left[\frac{\partial Q}{\partial(\beta Q(N-1))}\right]^{\mathrm{T}} \tilde{\beta} Q(N-1) + \\ &\left[\frac{\partial Q}{\partial(\gamma \boldsymbol{F}(N-1))}\right]^{\mathrm{T}} \tilde{\gamma}\boldsymbol{F}(N-1) + O_n\end{aligned} \tag{10}$$

Substituted Eq. (10) into Eq. (9), the higher-order term and the reconstruction error can be defined as:

$$\Psi = \tilde{W}\tilde{Q} + W^* O_n + \varepsilon_f \tag{11}$$

Based on the adaptive methods, the estimation value can be given by $\hat{\Psi}$ in Eq. (11). Combine the output of the regression neural network with the adaptive estimation value to form the estimation of the unknown part F in the model inverse. Therefore, through adaptive neural networks, the unknown part $\boldsymbol{F}(\boldsymbol{\eta},\dot{\boldsymbol{\eta}})$ in the model can be represented as

$$\hat{\boldsymbol{F}} = \hat{W}\Theta(\zeta,\hat{\alpha},\hat{\beta},\hat{\gamma}) + \hat{\Psi} \tag{12}$$

Assuming that the estimation error can satisfy the following conditions:

$$\left\|\boldsymbol{F} - \hat{\boldsymbol{F}}\right\| \le \sigma \left\|\bar{\zeta}_2 - \hat{\bar{\zeta}}_2\right\| \tag{13}$$

Where: σ is the normal number.

C. Sliding Mode Observer

For describing the unavailable velocity information, an adaptive neural network sliding mode observer is used to evaluate the speed status of the AUV, and the obtained velocity status variables could realize fault-tolerant control of the thruster.

Firstly, the intermediate variables for the unknown model can be given by:

$$\begin{aligned}&\zeta_1 = \boldsymbol{\eta},\quad \bar{\zeta}_2 = \dot{\boldsymbol{\eta}}\\ &\bar{\zeta} = \left[\zeta_1^{\mathrm{T}} \quad \bar{\zeta}_2^{\mathrm{T}}\right]^{\mathrm{T}},\quad \zeta = \left[\zeta_1^{\mathrm{T}} \quad \zeta_2^{\mathrm{T}}\right]^{\mathrm{T}}\end{aligned} \tag{14}$$

Through the state transformation model shown in [27], Eq. (3) can be described as:

$$\dot{\zeta} = \boldsymbol{A}\zeta + \bar{\boldsymbol{F}}(\zeta_1,\zeta_2) + \bar{\boldsymbol{G}}\boldsymbol{u} \tag{15}$$

$$\begin{aligned}&\boldsymbol{T} = \begin{bmatrix}\mathbf{I}_3 & 0\\ -\boldsymbol{T}_2 & \mathbf{I}_3\end{bmatrix},\ \boldsymbol{T}_2 = diag\{a_1 \quad a_2 \quad a_3\}\\ &\boldsymbol{A} = \begin{bmatrix}\boldsymbol{T}_2 & \mathbf{I}_3\\ -\boldsymbol{T}_2^{\,2} & -\boldsymbol{T}_2\end{bmatrix},\ \bar{\boldsymbol{F}}(\zeta_1,\zeta_2) = \begin{bmatrix}0\\ \boldsymbol{F}(\zeta_1,\bar{\zeta}_2)\end{bmatrix}\\ &\bar{\boldsymbol{G}} = \begin{bmatrix}0\\ \boldsymbol{G}(\zeta_1)\end{bmatrix},\ \zeta = \boldsymbol{T}\bar{\zeta},\ a_i \in R^+\end{aligned} \tag{16}$$

Based on Eq. (15), the sliding mode observer can be constructed and given by:

$$\begin{aligned}&\dot{\hat{\zeta}}_1 = \boldsymbol{T}_2\hat{\zeta}_1 + \hat{\zeta}_2 - \boldsymbol{L}_1\Delta_1 + \bar{\boldsymbol{P}}_1\varsigma_1\\ &\dot{\hat{\zeta}}_2 = -\boldsymbol{T}_2^{\,2}\hat{\zeta}_1 - \boldsymbol{T}_2\hat{\zeta}_2 + \boldsymbol{F}(\zeta_1,\hat{\zeta}_2) + \\ &\qquad \boldsymbol{G}(\zeta_1)\boldsymbol{u} - \boldsymbol{L}_2\Delta_1 + \bar{\boldsymbol{P}}_3\varsigma_1\end{aligned} \tag{17}$$

Where: $\bar{\boldsymbol{P}}$ is the inverse matrix of the positive-definite matrix $\boldsymbol{P}$, and the other variables are:

$$\boldsymbol{L}_1=\begin{bmatrix} l_{11} & & \\ & l_{12} & \\ & & l_{13}\end{bmatrix},\ \boldsymbol{L}_2=\begin{bmatrix} l_{21} & & \\ & l_{22} & \\ & & l_{23}\end{bmatrix}$$
$$\bar{\boldsymbol{P}}=\begin{bmatrix} \bar{\boldsymbol{P}}_1 & \bar{\boldsymbol{P}}_3 \\ \bar{\boldsymbol{P}}_3 & \bar{\boldsymbol{P}}_4\end{bmatrix},\ \Delta_1=\hat{\zeta}_1-\zeta_1 \tag{18}$$
$$\varsigma_1=\begin{cases} -\rho\|\boldsymbol{P}\|\dfrac{\Delta_1}{\|\Delta_1\|} & \|\Delta_1\|\neq 0 \\ 0 & \|\Delta_1\|=0\end{cases}$$

Then, the equivalent variable is defined as $\Delta_2=\hat{\zeta}_2-\zeta_2$, Eq. (19) can be obtained:

$$\begin{aligned}\dot{\Delta}_1&=(\boldsymbol{T}_2-\boldsymbol{L}_1)\Delta_1+\Delta_2+\boldsymbol{P}_1^{-1}\varsigma_1\\ \dot{\Delta}_2&=-(\boldsymbol{T}_2^{\,2}+\boldsymbol{L}_2)\Delta_1-\boldsymbol{T}_2\Delta_2+\\ &\hat{\boldsymbol{F}}(\zeta_1,\hat{\bar{\zeta}}_2)-\boldsymbol{F}(\zeta_1,\bar{\zeta}_2)+\boldsymbol{P}_3^{-1}\varsigma_1\end{aligned} \tag{19}$$

Meanwhile, a matrix variable is defined as:

$$\begin{aligned}\boldsymbol{A}_o&=\begin{bmatrix}\boldsymbol{T}_2-\boldsymbol{L}_1 & \mathbf{I}_3\\ -(\boldsymbol{T}_2^{\,2}+\boldsymbol{L}_2) & -\boldsymbol{T}_2\end{bmatrix}\\ \varphi&=diag\left\{0_3\quad \varepsilon_o\sigma^2\mathbf{I}_3\right\},\ \boldsymbol{T}_2<\boldsymbol{L}_1,\ \varepsilon_o\in R^+\end{aligned} \tag{20}$$

Through designing the diagonal matrix $\boldsymbol{L}_1,\boldsymbol{L}_2$, the variable $\boldsymbol{A}_0$ can turn into the Hurwitz matrix [27]. To any positive-definite matrix $\boldsymbol{Q}_0$, existing a positive-definite symmetric matrix $\boldsymbol{P}$ to realize

$$\boldsymbol{P}\boldsymbol{A}_o+\boldsymbol{A}_o^{\mathrm{T}}\boldsymbol{P}+\frac{1}{\varepsilon_o}\boldsymbol{P}\boldsymbol{P}+\varphi=-\boldsymbol{Q}_o \tag{21}$$

Prove.

By reselecting a Lyapunov function and constructing the integration variable as:

$$\boldsymbol{V}_1=\Delta^{\mathrm{T}}\boldsymbol{P}\Delta,\ \Delta=\left[\Delta_1^{\mathrm{T}}\quad \Delta_2^{\mathrm{T}}\right]^{\mathrm{T}} \tag{22}$$

$$\begin{aligned}\dot{\boldsymbol{V}}_1&=\dot{\Delta}^{\mathrm{T}}\boldsymbol{P}\Delta+\Delta^{\mathrm{T}}\boldsymbol{P}\dot{\Delta}\\ &=(\boldsymbol{A}_o\Delta)^{\mathrm{T}}\boldsymbol{P}\Delta+\Delta^{\mathrm{T}}\boldsymbol{P}\boldsymbol{A}_o\Delta+2\Delta^{\mathrm{T}}\boldsymbol{P}(\hat{\boldsymbol{F}}(\zeta_1,\hat{\zeta}_2)-\\ &\boldsymbol{F}(\zeta_1,\zeta_2))+2\Delta^{\mathrm{T}}\boldsymbol{P}\bar{\boldsymbol{P}}\left[\varsigma_1^{\mathrm{T}}\quad 0_3\right]^{\mathrm{T}}\end{aligned} \tag{23}$$

Combining with the Young's inequality and the assumed condition, Eq. (23) can be converted to:

$$\begin{aligned}&\forall:\ 2\boldsymbol{X}^{\mathrm{T}}\boldsymbol{Y}\le\frac{1}{\varepsilon}\boldsymbol{X}^{\mathrm{T}}\boldsymbol{X}+\varepsilon\boldsymbol{Y}^{\mathrm{T}}\boldsymbol{Y}\\ &\dot{\boldsymbol{V}}_1\le\Delta^{\mathrm{T}}(\boldsymbol{A}_o^{\mathrm{T}}\boldsymbol{P}+\boldsymbol{P}\boldsymbol{A}_o)\Delta+\frac{1}{\varepsilon_o}\Delta^{\mathrm{T}}\boldsymbol{P}\boldsymbol{P}\Delta+\\ &\varepsilon_o\sigma^2\Delta_2^{\mathrm{T}}\Delta_2-2\rho\|\boldsymbol{P}\|\|\Delta_1\|\le\Delta^{\mathrm{T}}\boldsymbol{Q}_o\Delta\end{aligned} \tag{24}$$

In viewpoint of Eq. (24), it can be known that the observer error Δ is able to converge to zero, which means that the observer can accurately estimate the velocity information and provide velocity estimation for the path tracking controller of the AUV.

Based on the LMI toolbox, the above matrix variables $\boldsymbol{P},\boldsymbol{L}_1,\boldsymbol{L}_2$ can be determined. The solution process is equivalent to solve a feasible element $\boldsymbol{P}>0$ to realize

$$\begin{aligned}&\begin{bmatrix}\boldsymbol{P}\boldsymbol{A}_0+\boldsymbol{A}_0^{\mathrm{T}}\boldsymbol{P}-\boldsymbol{M}\boldsymbol{C}-\boldsymbol{C}^{\mathrm{T}}\boldsymbol{M}^{\mathrm{T}}+\varphi & \boldsymbol{P}\\ \boldsymbol{P} & -\varepsilon_0\mathbf{I}_6\end{bmatrix}<0\\ &\boldsymbol{M}=\left[\boldsymbol{M}_1\quad \boldsymbol{M}_2\right]^{\mathrm{T}}=\boldsymbol{P}\left[\boldsymbol{L}_1^{\mathrm{T}}\quad \boldsymbol{L}_2^{\mathrm{T}}\right]^{\mathrm{T}},\boldsymbol{C}=\left[\boldsymbol{I}_3\quad 0_3\right]\end{aligned} \tag{25}$$

Where: $\boldsymbol{M}_1,\boldsymbol{M}_2$ are also the diagonal matrix.

D. Model Inverse Control

Different from the traditional model-based inversion control [28, 29], this section utilizes the adaptive regression neural network and sliding mode observer mentioned above to achieve fault-tolerant control when the velocity information is not available for AUV thrusters.

First the chosen sliding surface is given by:

$$s=\hat{\dot{e}}+2\Lambda e+\Lambda^2\int e\,\mathrm{d}t \tag{26}$$

Where: Λ is the normal number, $e=\boldsymbol{\eta}_R-\boldsymbol{\eta},\hat{\dot{e}}=\dot{\boldsymbol{\eta}}_R-\hat{\dot{\boldsymbol{\eta}}}$, and $\hat{\dot{\boldsymbol{\eta}}}$ can be obtained by the sliding mode observer given in Eq. (17), the model can be given by:

$$\hat{\dot{\boldsymbol{\eta}}}=\hat{\zeta}_2+\boldsymbol{T}_2\hat{\zeta}_1 \tag{27}$$

The virtual control instructions can be given by:

$$\ddot{\boldsymbol{\eta}}_{cmd}=\ddot{\boldsymbol{\eta}}_R+\Lambda^2 e+2\Lambda\dot{e}+ks \tag{28}$$

Where: k is also the normal number.

Theorem. If the AUV dynamic model in a current environment can be given by Eq. (1) and (3), the proposed fault-tolerant control model can be expressed as Eq. (29). By estimating the AUV velocity state through a sliding mode observer, the impact of current environment and thruster faults on path tracking control can be compensated, which ensures the AUV position error converge to zero.

$$\begin{aligned}&u=G(\eta)^+(\ddot{\eta}_{cmd}-\hat{F}(\eta,\hat{\dot{\eta}}))\\ &\dot{\hat{W}}=-\lambda_W s\hat{Q}^{\mathrm{T}},\quad \dot{\hat{\beta}}=-\lambda_\beta Q_\beta\hat{W}^{\mathrm{T}}sQ(N-1)^{\mathrm{T}}\\ &\dot{\hat{\alpha}}=-\lambda_\alpha Q_\alpha\hat{W}^{\mathrm{T}}s\zeta^{\mathrm{T}},\ \dot{\hat{\gamma}}=-\lambda_\gamma Q_\gamma\hat{W}^{\mathrm{T}}sf(N-1)^{\mathrm{T}}\\ &\dot{\hat{h}}=-\lambda_h s,\ \Psi=hs\end{aligned} \tag{29}$$

Prove.

By selecting the Lyapunov function, the velocity estimation can be given by:

$$\begin{aligned}\boldsymbol{V}_2=&0.5s^{\mathrm{T}}s+0.5tr(\tilde{W}\lambda_W^{-1}\tilde{W}^{\mathrm{T}})+0.5tr(\tilde{\alpha}^{\mathrm{T}}\lambda_\alpha^{-1}\tilde{\alpha})+\\ &0.5tr(\tilde{\beta}^{\mathrm{T}}\lambda_\beta^{-1}\tilde{\beta})+0.5tr(\tilde{\gamma}^{\mathrm{T}}\lambda_\gamma^{-1}\tilde{\gamma})+0.5\tilde{h}^{\mathrm{T}}\lambda_h^{-1}\tilde{h}\end{aligned} \tag{30}$$

$$
\begin{aligned}
\dot{V}_2 &= tr(\tilde{W}\lambda_W{}^{-1}\dot{\tilde{W}}^{\mathrm{T}})0.5tr(\dot{\tilde{\alpha}}^{\mathrm{T}}\lambda_\alpha{}^{-1}\tilde{\alpha}) + s^{\mathrm{T}}\dot{s} + \\
&\quad 0.5tr(\dot{\tilde{\beta}}^{\mathrm{T}}\lambda_\beta{}^{-1}\tilde{\beta}) + 0.5tr(\dot{\tilde{\gamma}}^{\mathrm{T}}\lambda_\gamma{}^{-1}\tilde{\gamma}) + 0.5\tilde{h}^{\mathrm{T}}\lambda_h{}^{-1}\dot{\tilde{h}} \\
&= tr(\tilde{W}\lambda_W{}^{-1}\dot{\tilde{W}}^{\mathrm{T}})0.5tr(\dot{\tilde{\alpha}}^{\mathrm{T}}\lambda_\alpha{}^{-1}\tilde{\alpha}) + \\
&\quad 0.5tr(\dot{\tilde{\beta}}^{\mathrm{T}}\lambda_\beta{}^{-1}\tilde{\beta}) + s^{\mathrm{T}}(\ddot{e} + 2\Lambda\dot{e} + \Lambda^2 e) + \\
&\quad 0.5tr(\dot{\tilde{\gamma}}^{\mathrm{T}}\lambda_\gamma{}^{-1}\tilde{\gamma}) + 0.5\tilde{h}^{\mathrm{T}}\lambda_h{}^{-1}\dot{\tilde{h}}
\end{aligned} \tag{31}
$$

Eq. (31) can be also given by:

$$
\begin{aligned}
\dot{V}_2 &= s^{\mathrm{T}}(\ddot{\eta}_R - \ddot{\eta} + 2\Lambda e + \Lambda^2 e - \Xi - \dot{\Xi}) - \\
&\quad tr(\tilde{W}\lambda_W{}^{-1}\dot{\hat{W}}^{\mathrm{T}}) - 0.5tr(\dot{\hat{\alpha}}^{\mathrm{T}}\lambda_\alpha{}^{-1}\tilde{\alpha}) - \\
&\quad 0.5tr(\dot{\hat{\beta}}^{\mathrm{T}}\lambda_\beta{}^{-1}\tilde{\beta}) - 0.5tr(\dot{\hat{\gamma}}^{\mathrm{T}}\lambda_\gamma{}^{-1}\tilde{\gamma}) - 0.5\tilde{h}^{\mathrm{T}}\lambda_h{}^{-1}\dot{\hat{h}}
\end{aligned} \tag{32}
$$

Where $\Xi = (\Delta_2 + T_2\Delta_1)$, and it has been proven in section 3.3 that this term will converge to zero.

Substituting Eq. (3), (28), and (29) into Eq. (32), then

$$
\begin{aligned}
\dot{V}_2 &= s^{\mathrm{T}}(\ddot{\eta}_R - (f + (\ddot{\eta}_R + \Lambda^2 e + 2\Lambda\dot{e} - \hat{f}(\eta,\hat{\eta}))) + \\
&\quad 2\Lambda e + \Lambda^2 e) - s^{\mathrm{T}}(\Xi + \dot{\Xi}) - tr(\tilde{W}\lambda_W{}^{-1}\dot{\hat{W}}^{\mathrm{T}}) - \\
&\quad 0.5tr(\dot{\hat{\alpha}}^{\mathrm{T}}\lambda_\alpha{}^{-1}\tilde{\alpha}) - 0.5tr(\dot{\hat{\beta}}^{\mathrm{T}}\lambda_\beta{}^{-1}\tilde{\beta}) - \\
&\quad 0.5tr(\dot{\hat{\gamma}}^{\mathrm{T}}\lambda_\gamma{}^{-1}\tilde{\gamma}) - 0.5\tilde{h}^{\mathrm{T}}\lambda_h{}^{-1}\dot{\hat{h}}
\end{aligned} \tag{33}
$$

And then, Substituting Eq. (9) and (19) into Eq (33), that is

$$
\begin{aligned}
\dot{V}_2 &= -tr(\tilde{W}\hat{Q}s^{\mathrm{T}}) - tr(\zeta s^{\mathrm{T}}\hat{W}Q_\alpha{}^{\mathrm{T}}\tilde{\alpha}) - \\
&\quad tr(Q(N-1)s^{\mathrm{T}}\hat{W}Q_\beta{}^{\mathrm{T}}\tilde{\beta}) - \\
&\quad tr(f(N-1)s^{\mathrm{T}}\hat{W}Q_\gamma{}^{\mathrm{T}}\tilde{\gamma}) - s\tilde{\Psi} - \\
&\quad tr(\tilde{W}\lambda_W{}^{-1}\dot{\hat{W}}^{\mathrm{T}}) - \frac{1}{2}tr(\dot{\hat{\alpha}}^{\mathrm{T}}\lambda_\alpha{}^{-1}\tilde{\alpha}) - \\
&\quad \frac{1}{2}tr(\dot{\hat{\beta}}^{\mathrm{T}}\lambda_\beta{}^{-1}\tilde{\beta}) - \frac{1}{2}tr(\dot{\hat{\gamma}}^{\mathrm{T}}\lambda_\gamma{}^{-1}\tilde{\gamma}) - \\
&\quad \frac{1}{2}\tilde{h}^{\mathrm{T}}\lambda_h{}^{-1}\dot{\hat{h}} - s^{\mathrm{T}}(\Xi + \dot{\Xi}) \\
\hbar &= Q_\alpha{}^{\mathrm{T}}\tilde{\alpha}\zeta + Q_\beta{}^{\mathrm{T}}\tilde{\beta}Q(N-1) + Q_\gamma{}^{\mathrm{T}}\tilde{\gamma}f(N-1)
\end{aligned} \tag{34}
$$

When the update rate is substituted into Eq.(34), and combining with the sliding observer error proof mentioned above, thereby:

$$\dot{V}_2 \le 0 \tag{35}$$

Stem from the Lyapunov stability theory, the effects of ocean current interference and unknown thruster faults can be effectively compensated based on the proposed observer based AUV path tracking control method， and can make the AUV position error converge to zero.

IV. SIMULATION ANALYSIS

The path tracking simulations were conducted on Omni Directional Intelligent Navigator AUV. Besides, the ODIN AUV has four identical thrusters on the horizontal plane, and its dynamic model has been studied and shown in [30] clearly.

Within the prescribed horizontal plane, the home position is $\boldsymbol{\eta} = [0.05, 0.05, 0.01]^{\mathrm{T}}$, and the home velocity is $\dot{\boldsymbol{\eta}} = [0,0,0]^{\mathrm{T}}$. By using first-order Gaussian Markov process to describe the ocean currents [22], the model can be given by:

$$\dot{V}_c + \mu V_c = \omega \tag{36}$$

Where: V_c is the amplitude of the ocean current in the reference coordinate system; ω is the Gaussian white noise with a mean value of -1.5 and a variance of 1; the constant term μ is set to 3; the current direction is π/4 in the reference coordinate system.

The initial parameters involved in the controller are set as follows:

$$
\begin{aligned}
&\omega_n = 3, \quad \xi = 0.8, \quad \lambda = \begin{bmatrix} 0 & & \\ & 0 & \\ & & 0.2 \end{bmatrix} \\
&\Lambda = \begin{bmatrix} 5 & & \\ & 5 & \\ & & 5 \end{bmatrix}, \quad \lambda_\Psi = \begin{bmatrix} 5 & & \\ & 5 & \\ & & 15 \end{bmatrix} \\
&\lambda_\alpha = \lambda_\beta = \lambda_\gamma = \lambda_W = \begin{bmatrix} 0.5 & & \\ & 0.5 & \\ & & 0.5 \end{bmatrix}
\end{aligned} \tag{37}
$$

The input layer nodes is set to 4, which responds to the heading angle information measured by the navigation sensor and the velocity information estimated from the sliding mode observer. The hidden-layer nodes is 6, and the output layer nodes is 3. The initial value of each of the weight variables is arbitrarily selected from [0, 0.5].

By using the LMI toolbox, the parameters involved in the sliding mode observer can be given by:

$$
\begin{aligned}
&\boldsymbol{T}_2 = diag(1.2, 1.2, 1.2) \\
&\boldsymbol{L}_1 = diag(3.7122, 3.7122, 3.7122) \\
&\boldsymbol{L}_2 = diag(-2.0383, -2.0383, -2.0383) \\
&\boldsymbol{\rho} = diag(0.2, 0.2, 0.2)
\end{aligned} \tag{38}
$$

The initial components are described as:

$$
\begin{aligned}
&\hat{\zeta}_1 = [0,0,0], \quad \hat{\zeta}_2 = [0,0,0] \\
&\boldsymbol{P} = \begin{bmatrix}
0.9760 & 0 & 0 & -0.6078 & 0 & 0 \\
0 & 0.9760 & 0 & 0 & -0.6078 & 0 \\
0 & 0 & 0.9760 & 0 & 0 & -0.6078 \\
-0.6078 & 0 & 0 & 1.1705 & 0 & 0 \\
0 & -0.6078 & 0 & 0 & 1.1705 & 0 \\
0 & 0 & -0.6078 & 0 & 0 & 1.1705
\end{bmatrix}
\end{aligned} \tag{39}
$$

In the ocean current environment, the ideal tracking path is an "8" shaped path and expressed as:

$$
\begin{aligned}
&\eta_d = [x_d, y_d, \phi_d], \quad x_d = 2\sin(0.5t) \\
&y_d = -2\cos(0.25t), \quad \phi_d = 0.1t
\end{aligned} \tag{40}
$$

Assuming that the first thruster occurs a 50% thrust loss ramp fault at the 20th second, and the fault would continue until the end of the experiment, the simulation function is given by:

$$k_{11} = \begin{cases} 0 & t < 20 \\ 0.5(1 - e^{-(t-20)/4}) & t \geq 20 \end{cases} \tag{41}$$

When a 50% thrust loss ramp fault occurs, Figure 2 to Figure 5 show the simulation results.

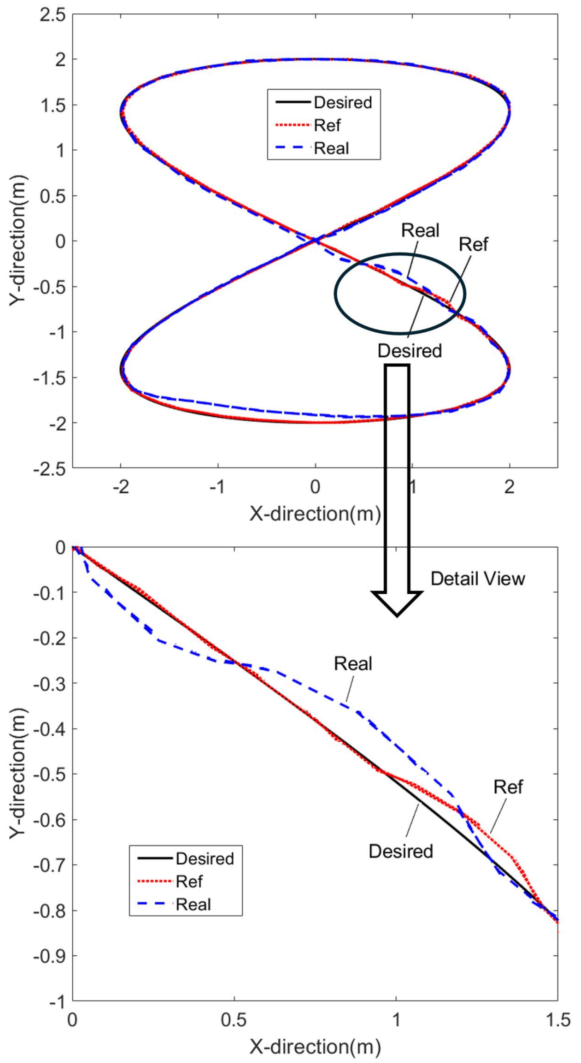

Fig. 2. AUV horizontal path

Figure 2 shows the desired path, the reference path after passing through the reference model, and the real path of the AUV. The changes in AUV control signals when considering thrust faults are shown in Figure 3. Then, due to the slow changes in thruster faults, the tracking ability of the AUV decreases, making it difficult to track the required path. However, the proposed method can modify the reference output path to meet the saturation constraint of the thruster.

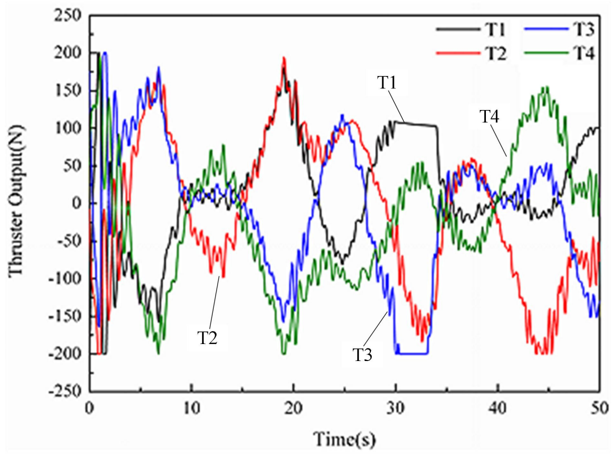

Fig. 3. AUV control signal

Figure 4 shows the AUV tracking errors in the overall simulation process, indicating that the error is still very small when the thruster fails (20 seconds). The average of the absolute errors is [0.0042m, 0.0031m, 0.0012rad] during the 3-DOF motion process, with the variance of [0.011m, 0.008m and 0.004rad]. Based on the proposed sliding mode observer, the AUV velocity can be well estimated in the reference coordinate system.

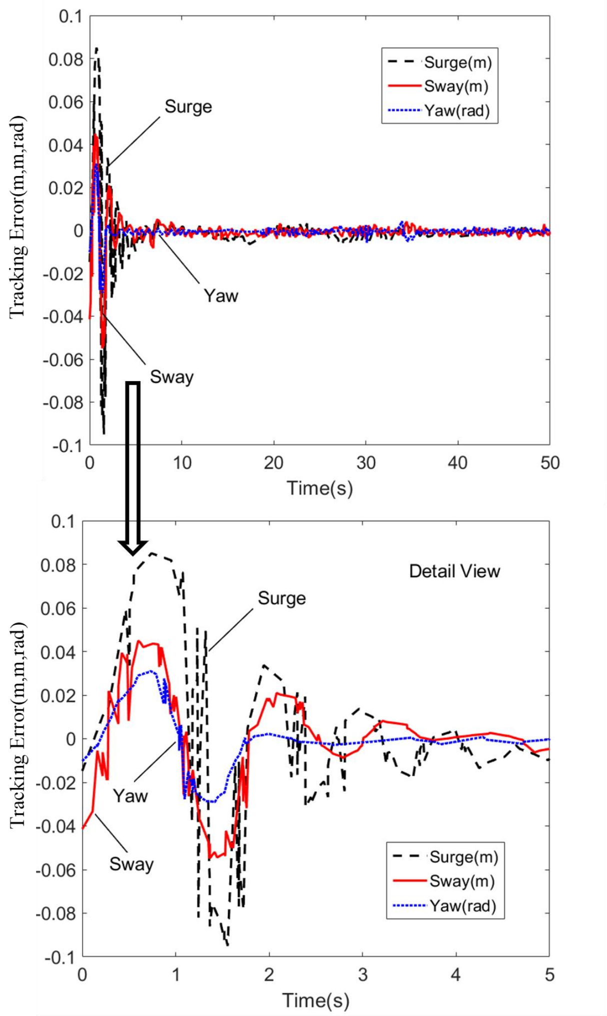

Fig. 4. AUV tracking error

Figure 5 shows the changing law of the state estimation parameters and actual values, and it can be concluded that although there are significant variations between the velocity estimation and the real values in the initial stage, the relative errors would reduce to zero quickly (about 3 seconds).

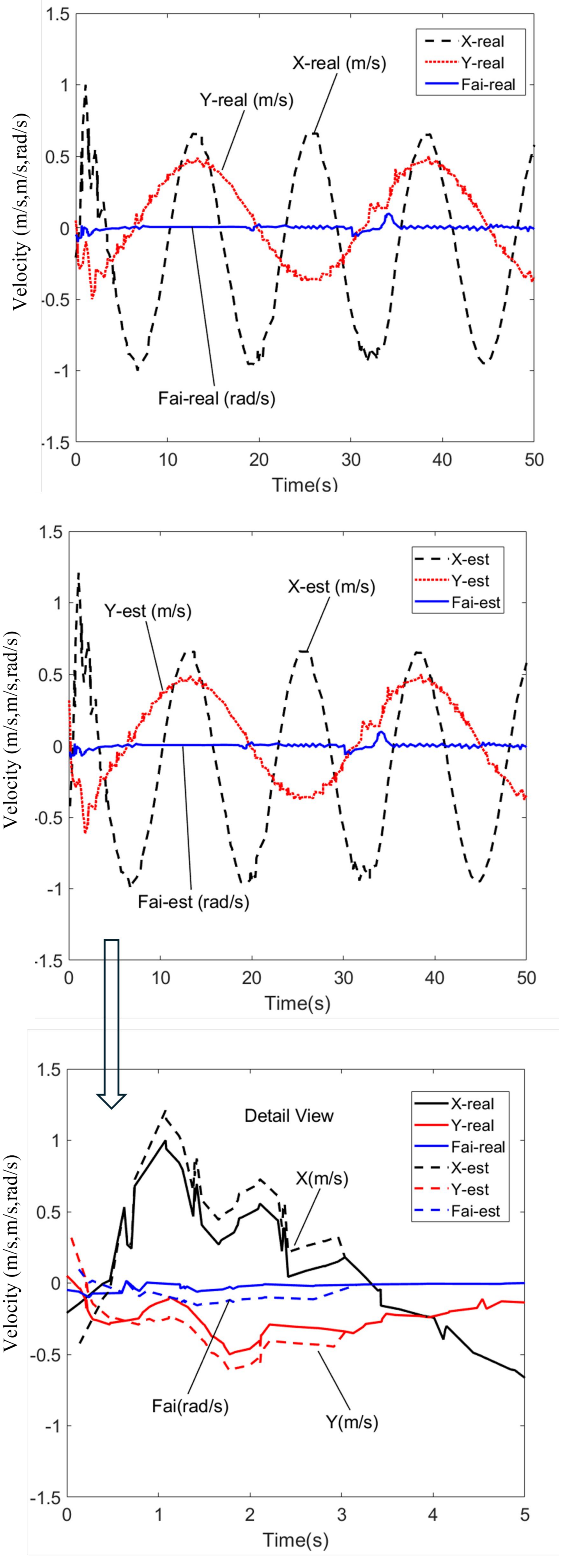

Fig. 5. State estimation parameters and actual values

Through the comparison results obtained from the conditions of no thruster faults and 50% slow thruster faults, the path tracking effectiveness is verified without the velocity feedback information, which can compensate for the sudden failure on AUV thrusters and achieve path tracking control under the saturation constraint of the thrusters.

V. Conclusion

To achieve highly reliable AUV path tracking control when considering the ocean current interference and thruster saturation constraints conditions, a fault-tolerant control method for AUV thrusters without velocity feedback is proposed. Besides, the adaptive regression neural networks is used to estimate the unknown AUV dynamic models, which avoids the changes in dynamic characteristics caused by the thruster faults and the limitations of traditional model inverse control methods. Meanwhile, the proposed method does not involve the AUV velocity measurement information, thus avoiding the sensor failures or the large measurement error problem in the path tracking process. The simulation results show that the sliding mode observer can accurately estimate the AUV velocity` state, thereby effectively compensating for the impact of thruster faults. Through the path reference output and the thruster output signal, the proposed method can adjust the reference path to achieve path tracking control under saturation constraint of the thrusters.

References

[1] Huang, D., Li, Y., Yu, J.C., Li, S. and Feng, X.S., "State-of-the-art and Development Fiends of AUV Intelligence." Robot, Vol. 42, no. 2, pp.215-231, 2020.

[2] Guerrero, Jesús, Ahmed Chemori, Jorge Torres, and Vincent Creuze. "STA-based design of an adaptive disturbance observer for autonomous underwater vehicles: From concept to real-time validation." *Control Engineering Practice* ,2024 Mar 1;144:105831.

[3] Ahmed, F., **ang, X., Jiang, C., **ang, G. and Yang, S., "Survey on traditional and AI based estimation techniques for hydrodynamic coefficients of autonomous underwater vehicle. " Ocean Engineering, 268, pp.113300,2023.

[4] Chen T., et al. "Imitation learning from imperfect demonstrations for AUV path tracking and obstacle avoidance." Ocean engineering, vol. 298, no. Apr.15, Jan. 2024, pp. 1.1-1.12.

[5] Jialei Zhang, et al. "Adaptive Saturated Path Following Control of Underactuated AUV With Unmodeled Dynamics and Unknown Actuator Hysteresis." IEEE transactions on systems, man, and cybernetics. Systems, vol. 53, no. 10 Pt.1, Jan. 2023, pp. 6018-6030. http://dx.chinadoi.cn/10.1109/TSMC.2023.3280065

[6] Liu, H.T., Zhou, J.Y., Tian, X.H. and Mai, Q.Q., "Finite-time Self-structuring Neural Network Trajectory Tracking Control of Underactuated Autonomous Underwater Vehicles." Ocean Engineering, Vol. 268, pp. 113450, 2023.

[7] Gong H, Er MJ, Liu Y. Fuzzy adaptive optimal fault-tolerant trajectory tracking control for underactuated AUVs with input saturation. Ocean Engineering. 2024 Nov 1;311:118940.

[8] Tijjani AS, Chemori A, Creuze V. A survey on tracking control of unmanned underwater vehicles: Experiments-based approach. Annual Reviews in Control. 2022 Jan 1; 54:125-47.

[9] Karimi HR, Lu Y. Guidance and control methodologies for marine vehicles: A survey. Control Engineering Practice. 2021 Jun 1; 111:104785.

[10] K. Ishaque, S. S. Abdullah, S. Ayob, and Z. Salam, "A simplified approach to design fuzzy logic controller for an underwater vehicle," *Ocean Engineering,* vol. 38, no. 1, pp. 271-284, 2011.

[11] Bateman, A., Hull, J. and Lin, Z., "A Backstepping-based Low-and-high Gain Design for Marine Vehicles." International Journal of Robust and Nonlinear Control, Vol. 19, no. 4, pp. 480-493,2009.

[12] Zhang, T., Li, D.J., Peng, S.L., Xia, Q.C., and Yang, C.J., "Research on Terminal Docking of Autonomous Underwater Vehicle Based on Visual Guidance and Rotational Docking Station." Journal of Mechanical Engineering, Vol. 54, no. 20, pp. 81-88,2018.

[13] Li, J., **ang, X., Dong, D. and Yang, S., Prescribed time observer based trajectory tracking control of autonomous underwater vehicle with tracking error constraints. Ocean Engineering, 274, p.114018,2023.

[14] Liu, X., Zhang, M.J., Yao, F. and Chu, Z.Z., "Observer-based Region Tracking Control for Underwater Vehicles without Velocity Measurement." Nonlinear Dynamics, Vol. 108, no. 4, pp.3543-3560,2022.

[15] Liu, T., Li, J., Zhang, G., Su, Z. and Wang, X., "Distributed observer position-based event-triggered formation control for unmanned surface vessels with confined inter-event times. " *Ocean Engineering*, *296*, p.116884,2024.
[16] Su, B., Wang, H. B. and Wang, Y.L., "Dynamic Event-triggered Formation Control for AUVs with Fixed-time Integral Sliding Mode Disturbance Observer." Ocean Engineering, Vol. 240, pp. 109893,2021.
[17] Wang, Y.Y., Chen, J.W. and Gu, L.Y., "Output Feedback Fractional-order Nonsingular Terminal Sliding Mode Control of Underwater Remotely Operated Vehicles." The Scientific World Journal, pp. 838019,2014.
[18] Corradini, M.L. and Orlando, G., "A Robust Observer-based Fault Tolerant Control Scheme for Underwater Vehicles." Journal of Dynamic Systems, Measurement, and Control, Vol. 136, no. 3, pp.034504,2014.
[19] Zhang, M. J. and Chu, Z.Z., "Adaptive Sliding Mode Control Based on Local Recurrent Neural Networks for Underwater Robot." Ocean Engineering, Vol. 45, pp. 56-62,2012.
[20] Avila, J.P.J., Donha, D.C. and Adamowski, J.C., "Experimental Model Identification of Open-frame Underwater Vehicles." Ocean Engineering, Vol. 60, pp.81-94,2013.
[21] Soylu, S., Buckham, B.J. and Podhorodeski, R. P., "A Chattering-Free Sliding-mode Controller for Underwater Vehicles with Fault-tolerant Infinity-norm Thrust Allocation." Ocean Engineering, Vol. 35, no. 16, pp.1647-1659,2008.
[22] Fossen, T. I., "Handbook of marine craft hydrodynamics and motion control." United Kingdom: John Wiley & Sons, 2011.
[23] Magueresse A., and Badia S.. "Adaptive quadratures for nonlinear approximation of low-dimensional PDEs using smooth neural networks[Formula presented]." Computers & Mathematics with Applications: An International Journal, vol. 162, no. May 15, Jan. pp. 1-21,2024.
[24] Wenxing Zhu, and Lihui Wang. "Adaptive finite-time fault-tolerant control for Robot trajectory tracking systems under a novel smooth event-triggered mechanism." Proceedings of the Institution of Mechanical Engineers, Part I. Journal of Systems and Control Engineering, vol. 238, no. 2, Jan. pp. 288-303, 2024.
[25] Yuan, Jian , et al. "An Underwater Thruster Fault Diagnosis Simulator and Thrust Calculation Method Based on Fault Clustering." Journal of Robotics , 2021.
[26] Lin, F.J., Chen, S.Y. and Shyu, K.K., "Robust Dynamic Sliding-Mode Control Using Adaptive RENN for Magnetic Levitation System." IEEE Transactions on Neural Networks, Vol. 20, no. 6, pp.938-951, 2009.
[27] Tan, C.P., Yu, X.H. and Man, Z.H., "Terminal Sliding Mode Observers for a Class of Nonlinear Systems." Automatica, Vol. 46, no. 8, pp. 1401-1404, 2010.
[28] Kim, B.M., Kim, B.S. and Kim, N.W., "Trajectory Tracking Controller Design Using Neural Networks for a Tiltrotor Unmanned Aerial Vehicle." Proceedings of the Institution of Mechanical Engineers, Part G: Journal of Aerospace Engineering, Vol. 224, no. 8, pp. 881-896, 2010.
[29] Peng, C., Wang, X.M. and Chen, X., Design of tiltrotor flight control system in conversion mode using improved neutral network PID. Advanced Materials Research, 850, pp.640-643, 2014.
[30] Li Z , Wang M , Ma G ,et al. Adaptive reinforcement learning fault-tolerant control for AUVs With thruster faults based on the integral extended state observer. Ocean Engineering, 2023.

Xiu-lian Liu received her PHD degree in Mechanical Design and Theory from Harbin Engineering University in 2018. Moreover, her main research direction is mechanical design and theory, nonlinear systems control. Now, she serves as a Lecturer in Huzhou Vocational & Technical College.

Li-xin Yang received her PHD degree in system engineering from Harbin Engineering University in 2012. Her main research direction is signal processing, nonlinear systems control. Now, she serves as a Lecturer in Huzhou Vocational & Technical College.

Li-dong Guo received his PHD degree in Navigation, Guidance and Control from Harbin Engineering University in 2011. His main research direction is nonlinear systems control, navigation system automation technology. Now, he serves as a Lecturer in Huzhou Vocational & Technical College.

Jian-wei Zhu received his PHD degree in Process Equipment and Control Engineering from Zhejiang University of Technology in 2016. His main research direction is Structural integrity assessment. Now, he serves as an Associate Professor in Huzhou Vocational & Technical College.

Qi-qi Shen received his MS degree in Mechanical Design and Theory from Zhejiang Sci-Tech University in 2011. Currently, His main research direction is industrial automation. Now, he serves as an Assistant in Huzhou Vocational & Technical College.